Int J Thermophys (2010) 31:1685–1695
DOI 10.1007/s10765-010-0816-7

The Immersion Characteristics of Industrial PRTs

D. R. White · C. L. Jongenelen

Received: 8 March 2010 / Accepted: 20 August 2010 / Published online: 14 September 2010

Abstract Immersion effects are one of the most significant sources of error in the use of industrial platinum resistance thermometers (IPRTs). This article combines the development of a mathematical model of immersion error and experimental measurements of the immersion characteristics of a range of IPRTs immersed in different fluids at different temperatures. The mathematical model relates the relative temperature error in the thermometer indication to two exponential terms, with one of the 1/e decay lengths three times the other. The experimental results show that both of the exponential terms are important for shallow immersion, but one is sufficient for long immersion. The decay length for the thermometers depends on the diameter of the probe and on the thermal environment into which it is immersed. For the thermometers evaluated here in mineral oil, silicon oil, and molten salt, the 1/e decay length is about three to four times the diameter of the thermometers. A simple rule of thumb for ensuring adequate immersion in calibration baths is developed.

Keywords Immersion · Platinum resistance thermometer · Temperature

1 Introduction

Immersion effects are one of the most significant sources of error in the use of industrial platinum resistance thermometers (IPRTs). The error arises because the thermometer provides a thermal connection between two zones at different temperatures, and the resulting heat flow through the thermometer affects the temperature at the

D. R. White (✉) · C. L. Jongenelen
Measurement Standards Laboratory of New Zealand, Industrial Research Limited,
P.O. Box 31310, Lower Hutt 5040, New Zealand
e-mail: r.white@irl.cri.nz

location of the sensor. In most calibration laboratories, the immersion problem is avoided completely by immersing the thermometers as much as practical into the calibration medium. However, there are occasions when, because of physical constraints, immersion effects become significant. These cases include when the IPRTs are unusually short, when dry-block calibrators are used, or when fixed-point cells are used.

Theoretical models of the immersion error have been developed for thermometers [1,2], for industrial thermometer wells [3], and for the analogous problem associated with the effectiveness of heat-sink fins [4,5]. However, the utility of the models is limited due to the dependence on surface heat transfer coefficients, properties that are highly dependent on thermal conductivities and flow within the medium where the thermometer is immersed. The purpose of this article is to confirm the mathematical models of the immersion effect, to confirm the key influence variables, and to develop a useful rule of thumb for managing immersion errors in calibration baths. First, in Sect. 2, the article develops a mathematical model of thermometer immersion from which two simple expressions for immersion error are derived. Section 3 presents measurements of the immersion characteristics of IPRTs of different diameter, in different media, and at different temperatures. Least-squares fits of the model equations to the measurements confirm the general validity of the model and highlight the long 1/e decay length associated with immersion in typical calibration-bath fluids. Finally, Sect. 4 summarizes the results and draws some conclusions.

2 Mathematical Model

This section derives a simple one-dimensional model of thermometer immersion. The derivation follows a line of reasoning common to other derivations related to thermometers, thermowells, and heat-sink fins, [1,2,4–6] except that the boundary conditions are more appropriate to the calibration of IPRTs. Figure 1 shows a simplified diagram of the situation in which a cylindrical thermometer is immersed in two different media: the medium on the left is typically air (subscript a), and that on the right is the calibration medium (subscript s), which might be the fluid of a calibration bath, a fixed-point cell, or the well of a dry block. For simplicity, it is assumed that the thermometer is relatively thin so that the temperature in the thermometer is purely a function of length, i.e., the temperature distribution across a small elemental section of the thermometer is uniform. This assumption allows the use of the one-dimensional Fourier equation for heat flow. Within the medium on the right of Fig. 1, which is the system of interest, the temperature profile along the thermometer, $T(x)$, must satisfy [5]

$$kA\frac{\mathrm{d}^2T(x)}{\mathrm{d}x^2} + h_{\mathrm{s}}C(T_{\mathrm{s}} - T(x)) = 0, \tag{1}$$

where k is the axial thermal conductivity of the material from which the thermometer is made, A and C are respectively, the cross-sectional area and circumference

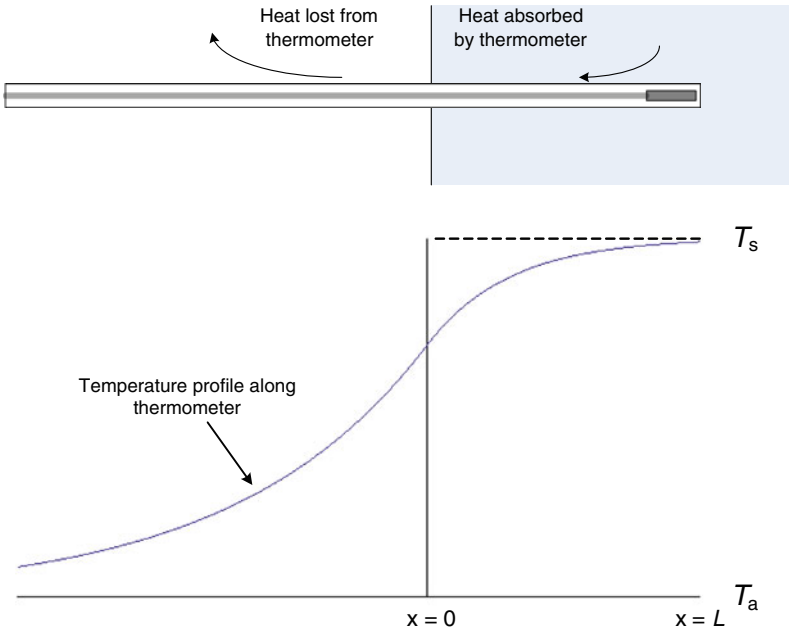

Fig. 1 Simplified diagram of the thermometer immersed in the system of interest and the corresponding temperature profile along the thermometer

of the thermometer, h_s is the surface heat transfer coefficient between the calibration medium and the thermometer, and T_s is the temperature of the calibration medium. In the left-hand medium, the air above the calibration medium in Fig. 1, a similar equation is satisfied:

$$kA\frac{d^2T(x)}{dx^2} + h_aC(T_a - T(x)) = 0. \tag{2}$$

Eq. 1 can be simplified by making the substitutions $\theta_s(x) = T(x) - T_s$, and

$$m_s^2 = 4h_s/kD, \tag{3}$$

where D is the diameter of the thermometer. Hence,

$$\frac{d^2\theta_s(x)}{dx^2} - m_s^2\theta_s(x) = 0, \tag{4}$$

and there is a similar equation (differing only in subscripts) for the temperature in that part of the thermometer exposed to the air. Both the equations have general solutions of the form,

$$\theta_s(x) = A_s \exp(m_s x) + B_s \exp(-m_s x). \tag{5}$$

The solution of the two equations, with a total of four unknown parameters, requires the imposition of four boundary conditions. Since the temperature, $T(x)$, and its derivative must be continuous at the boundary between the two media ($x = 0$), two of the boundary conditions are straight forward:

$$A_\mathrm{s} + B_\mathrm{s} + T_\mathrm{s} = A_\mathrm{a} + B_\mathrm{a} + T_\mathrm{a}, \tag{6}$$

and

$$m_\mathrm{s}(A_\mathrm{s} - B_\mathrm{s}) = m_\mathrm{a}(A_\mathrm{a} - B_\mathrm{a}). \tag{7}$$

The remaining two boundary conditions are determined from the heat flow at the two ends of the thermometer. For the end of the thermometer exposed to the air, it is assumed that the thermometer, with lead wires, is long enough to ensure that the thermometer temperature converges on T_a, or equivalently,

$$\theta_\mathrm{a}(x)|_{x=-\infty} = 0, \tag{8}$$

which leads to $B_\mathrm{a} = 0$.

For the end of the thermometer immersed in the system of interest, it is assumed that there is some heat flowing into the end of the thermometer, dependent on the temperature difference between the thermometer and the system. This heat flow must induce a gradient in the thermometer temperature at the tip so that

$$kA \left.\frac{\mathrm{d}\theta_\mathrm{s}}{\mathrm{d}x}\right|_{x=L} = -h_\mathrm{e} A \theta_\mathrm{s}(L), \tag{9}$$

where h_e is the surface heat transfer coefficient for the end of the thermometer. Once all the boundary conditions are applied, the temperature profile along the thermometer within the system of interest is found to be

$$T(x) = T_\mathrm{s} + \frac{(T_\mathrm{a} - T_\mathrm{s}) m_\mathrm{a} \left[(h_\mathrm{e} - k m_\mathrm{s}) \exp\left(m_\mathrm{s}(x - L)\right) + (h_\mathrm{e} + k m_\mathrm{s}) \exp\left(-m_{\mathrm{s(x-L)}}\right) \right]}{(m_\mathrm{a} + m_\mathrm{s})(h_\mathrm{e} + k m_\mathrm{s}) \exp\left(m_\mathrm{s} L\right) - (m_\mathrm{a} - m_\mathrm{s})(h_\mathrm{e} - k m_\mathrm{s}) \exp\left(-m_\mathrm{s} L\right)}. \tag{10}$$

For the temperature at the location of the sensor ($x = L$), this simplifies to

$$T(L) = T_\mathrm{s} + \frac{2(T_\mathrm{a} - T_\mathrm{s}) m_\mathrm{a} h_\mathrm{e}}{(m_\mathrm{a} + m_\mathrm{s})(h_\mathrm{e} + k m_\mathrm{s}) \exp\left(m_\mathrm{s} L\right) - (m_\mathrm{a} - m_\mathrm{s})(h_\mathrm{e} - k m_\mathrm{s}) \exp\left(-m_\mathrm{s} L\right)}. \tag{11}$$

Note that some heat flow at the end, characterized by a non-zero value for h_e, is necessary for the temperature error to occur. In addition to real end effects, the h_e parameter also accounts for the fact that the sensor is distributed over a region extending up to 30 mm or more from the tip of the thermometer.

For relatively large immersions where $\exp(m_s L) \gg \exp(-m_s L)$, the expression for the error simplifies to

$$T(L) \approx T_s + (T_a - T_s)\frac{2m_a h_e}{(m_a + m_s)(h_e + km_s)} \exp(-m_s L). \tag{12}$$

For the purposes of the analysis in Sect. 3, it is sufficient for Eq. 12 to be parameterized as

$$\frac{T_s - T(x)}{T_s - T_a} \approx K \exp(-L/L_0), \tag{13}$$

which relates the relative temperature error to a simple exponential function that is nominally independent of temperature (so long as L_0 and K are independent of temperature). Equation 13 also highlights the 1/e decay length, L_0, which characterizes the exponential decrease in immersion error with increasing immersion.

At lesser immersion, where $\exp(-m_s L)$ is less than $\exp(m_s L)$ but not small enough to be neglected, Eq. 11 is approximated by

$$T(L) \approx T_s + \frac{2(T_a - T_s)m_a h_e}{(m_a + m_s)(h_e + km_s)} \exp(-m_s L) \times \left[1 + \frac{(m_a - m_s)(h_e - km_s)}{(m_a + m_s)(h_e + km_s)} \exp(-2m_s L)\right], \tag{14}$$

or more simply:

$$\frac{T_s - T(x)}{T_s - T_a} \approx K_1 \exp(-L/L_0) + K_2 \exp(-3L/L_0), \tag{15}$$

which shows that the immersion characteristic has two exponential terms, with one that decays at three times the rate of the other.

The most important parameter of Eqs. 12 and 14 is m_s, which determines the 1/e decay length,

$$L_0 = \sqrt{kD/4h_s}, \tag{16}$$

for the propagation of thermal influences along the thermometer. Ideally, for good thermometer immersion characteristics, L_0 should be small, suggesting a thermometer with a small diameter, D, low thermal conductivity, k, and a high surface heat transfer coefficient, h_s, in the system of interest.

Because the thermometer diameter and conductivity are common to both m_s and m_a, one of the factors in Eqs. 12 and 14 simplifies and depends only on the relative values of the surface heat transfer coefficients in air and the system:

$$\frac{m_a}{(m_a + m_s)} = \frac{h_a^{1/2}}{h_a^{1/2} + h_s^{1/2}}. \tag{17}$$

In general, the surface heat transfer coefficients, h_s, h_a, and h_e, are not calculable from first principles. In fluids they are associated with flow and boundary layers, and therefore depend on the flow velocity, whether the flow is normal or axial, and may depend on Reynolds, Prandtl, and Nusselt dimensionless numbers [5]. References [3] and [5] give the correlations for the dimensionless numbers for fluid flow normal to the axis of the thermometer, but not for axial flow, which is the case usually relevant to thermometer calibration.

Kerlin and Shepard [1] and Benedict and Murdock [3] derive versions of Eq. 12 with different boundary conditions appropriate for metal thermowells. Their model suggests a slight change in parameterization that might give a more realistic model of thermocouples and industrial platinum resistance thermometers, which are usually manufactured from a stainless steel tube. They note that the axial conduction depends on the cross-sectional area of a metal tube (in Eq. 2), $A = \pi(r_o^2 - r_i^2)$, where r_o and r_i are, respectively, the outer and inner radii of the tube. For a thin-walled tube with $r_o - r_i = \Delta r$, the 1/e decay length, becomes

$$L_0 = \sqrt{k\Delta r/h_s}, \tag{18}$$

which is now dependent on the thickness of the thermometer sheath rather than its diameter (compare with Eq. 16).

A further complication, not considered here, is the additional heat transfer by radiation, which must be considered for high-temperature measurements (>400 °C). The radiation effects lead to a non-linear differential equation that must be solved numerically and is not readily amenable to least-squares fits [3].

3 Experimental Results

3.1 Experimental Design and Analysis

Five stainless-steel sheathed IPRTs of diameters 3.0 mm, 4.5 mm, 6.35 mm, 7.94 mm, and 9.53 mm were manufactured using the same model of sensing element, a 15 mm long partially supported wire-wound 100 Ω sensor. The immersion characteristics of the five thermometers were measured in mineral oil, silicon oil, and molten salt at temperatures ranging from −20 °C to 220 °C. For the temperature ranges surveyed here, the uniformity and stability of the baths were all within 0.5 mK.

The measured immersion characteristics were analyzed using non-linear least-squares fits to Eq. 13 or 15, which relate the relative temperature error to either one or two exponential functions. At large immersions, the data is expected to follow a straight line on a semilog plot, with the slope of the line giving the value for $-1/L_0$.

Some care is required with the least-squares fit. In addition to the multiple solutions and sensitivity to starting values typical of non-linear fits, there are other problems. First, the models are not capable of resolving independent values for the T_a and K constants. For example, in Eq. 13, any combination of T_a and K values that yield the same value of $(T_s - T_a)K$ all give the same fit. For this reason, T_a was assumed to be 20 °C in all fits. The fitted values of K_1 and K_2 are, therefore, dependent on this

assumption, but the fitted values of L_0 and T_s are independent of the assumption. Note that a fitted value for T_s is required to infer values for the immersion errors.

Some care is required in the selection of points for analysis, and typically points at the beginning and end of the immersion characteristic have to be removed for different reasons. First, the temperature sensor is 15 mm long and located at a range of positions near $x = L$, rather than exactly at $x = L$ as assumed in the model. This has the effect of smearing the immersion characteristic, especially for the small-diameter thermometers with a small L_0 value. Secondly, the model (Eq. 13) assumes $\exp(m_s L) \gg \exp(-m_s L)$, and this is not the case for small immersions. Finally, and especially for the salt-bath data, the transition from ambient temperature to system temperature is not a step function as assumed in the derivation of Eq. 10. For all these reasons, measurements at small immersions show a departure from the simple exponential model (Eq. 13) and, to a lesser degree, also from Eq. 15. At the other end of the characteristics, near maximum immersion, the immersion error, $T_s - T(L)$, is sufficiently small to be undetectable against the fluctuations in the bath temperature.

The final complication with the least-squares fit relates to the range of the data, which span more than three decades. To ensure that all points contribute equally to the fit, a weighting must be applied. It was assumed that the relative uncertainty in the measured value of the immersion error at each point was similar. For the simple model (Eq. 13), this is equivalent to assuming a constant uncertainty for all the measured values of L, and the fit was weighted accordingly. The same weighting was used for the fits to the more complex model (Eq. 15).

3.2 Experimental Results

Figure 2 plots the measured immersion characteristic for the 7.94 mm diameter IPRT immersed in silicon oil at 120 °C, and shows clearly the contributions of the two

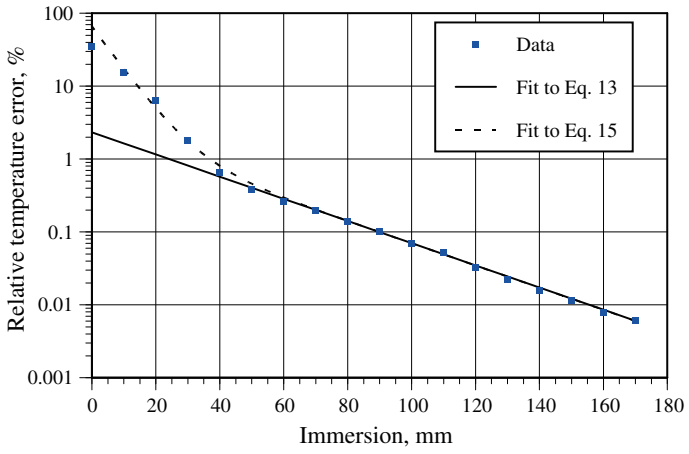

Fig. 2 Immersion characteristic for the 7.94 mm diameter stainless-steel sheathed IPRT in silicon oil at 120 °C

exponential terms of Eq. 15. The solid curve shows the least-squares fit using a single exponential function (Eq. 13). To get a good quality fit to Eq. 13, the measured points below 60 mm immersion had to be removed from the dataset. When the additional exponential term was added to the fitted function (the dotted curve), and all data were included in the fit, the values for the previously fitted parameters (T_s, L_0, and K_1) remained the same within the uncertainties of the fits. Note, to plot the measured data, it is necessary to use the value for T_s determined from the fit.

Most of the measured immersion characteristics showed a departure from the single exponential function at low immersions consistent with the contribution of the second exponential term of Eq. 15. Immersion characteristics measured in the molten salt bath (220 °C) for the 3 mm and 4.5 mm IPRTs did not support the inclusion of the second exponential term. However, the salt bath is constructed with a layer of insulation, a protective metal shield and a 10 mm to 20 mm air space over the salt so that the immersion characteristic at short immersions is expected to be inconsistent with the model, which assumes a step change in temperature. For this reason, the salt-bath data have been removed from some of the following analyses.

The effect of the second exponential terms was most pronounced for the larger diameter probes, which gave fits similar to Fig. 2. In some of the characteristics for the 3 mm and 4.5 mm diameter probes, the contribution of the second exponential was apparent only in the points at 10 mm and 20 mm, and the error at 0 mm immersion (with the probe just touching the surface of the oil) was increased, probably by the smearing effect of the distributed sensing element.

Ideally, if the surface heat transfer coefficients and thermal conductivities are the same at all temperatures, then the immersion characteristic should be the same at all temperatures. This is illustrated in Fig. 3, which shows the immersion characteristic for a 4.5 mm diameter IPRT in a dry-block calibrator, measured at three different temperatures, −40 °C, 0 °C, and 50 °C. Most importantly, when expressed in terms of relative temperature errors, as suggested by Eq. 13, all the three curves are very similar. Note that immersion in Fig. 3 is measured from the bottom of the dry block, and that only the lowest 60 mm of data are given.

Figure 4 shows the measured immersion characteristics for the 4.5 mm IPRT for the five sets of measurements in the oil baths. The greater consistency of the characteristics for the dry-block tests suggests that there are real changes in the surface heat transfer coefficients in different oil baths, and at different temperatures in the oils. Figure 5, which summarizes the L_0 values determined from all the immersion measurements for all the five probes, also suggests that other factors apply. The variability in the measured L_0 values greatly exceeds the uncertainty in the values determined from the fits, and there is no consistent pattern for the 6.35 mm, 7.94 mm, and 9.53 mm probes. Some variability is expected because the surface heat transfer coefficients depend on thermal boundary layers, which in turn depend on temperature and flow rates. The main cause of the variability is probably due to the effects of adjacent structures within the baths, such as walls and neighboring thermometers, which influence the flow and formation of boundary layers around the thermometers. Additionally, there was probably some variation in the placement of the probes in the different baths and temperatures (this factor was not controlled or recorded).

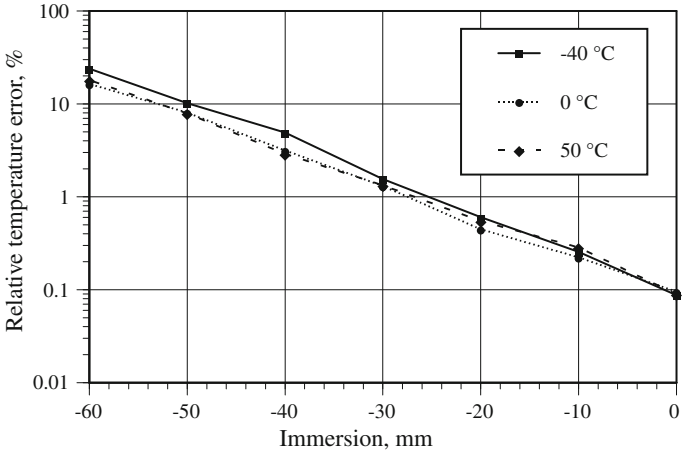

Fig. 3 Immersion characteristics for a 4.5 mm stainless steel sheathed IPRT at three different temperatures in dry-block calibrator with 5 mm diameter holes. Only data from the lowest 60 mm of immersion are shown so that 0 mm immersion corresponds to full immersion. The 1/e decay length for all the three curves is close to 11 mm

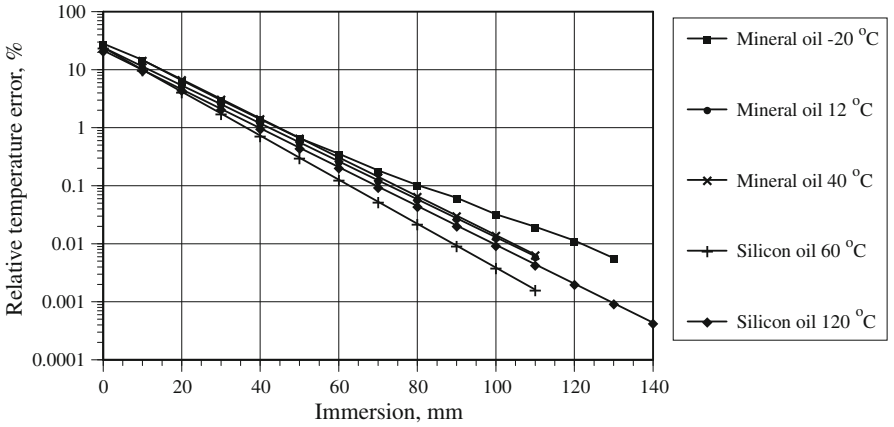

Fig. 4 Immersion characteristics for 4.5 mm diameter thermometer in different oil baths and at different temperatures

One surprising result of the measurements is that the 1/e decay lengths for the thermometers seemed to be consistent across the three different bath fluids, mineral oil, silicon oil, and nitrate salt. However, given that the thermal conductivities, specific heats, and viscosities of the three fluids are similar, it can probably be expected that the surface heat transfer coefficient for the three media will also be similar.

One of the notable features is that the 1/e decay lengths for the thinner thermometers, for which the measurements seemed to be more consistent, were about four times the diameters of the thermometers. This was significantly longer than observed in the dry-block calibrator where the decay length for a 4.5 mm probe was close to 11 mm,

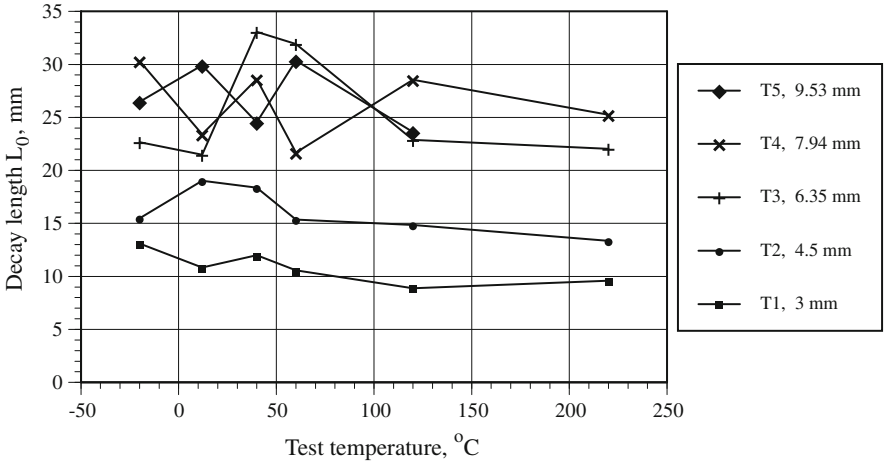

Fig. 5 Fitted values for the 1/e decay length L_0 for all the different immersion characteristics. Measurements at the temperatures −20 °C, 12 °C, and 40 °C are in a mineral oil bath, 60 °C and 120 °C in a silicon oil bath, and 220 °C in a salt bath

about 2.5 times the diameter. This suggests that the surface heat transfer coefficient in an aluminum block with heat-sink grease is better than that in a well-stirred oil bath.

One of the reasons for carrying out the immersion tests was to develop some simple rules of thumb for ensuring adequate immersion during routine calibrations. To investigate a variety of rules, all the immersion data, except for those in the salt bath, were plotted on a single graph as a function of different variables. The data were plotted against immersion normalized according to the decay lengths L_0, the diameter, square root of diameter, tube wall thickness (see Eq. 18), and square root of tube wall thickness. The graph that gave the least dispersion was the plot against diameter, as shown in Fig. 6. Also shown in Fig. 6 is a two-segment line that gives an approximate upper bound to the relative temperature error. The first segment of the line gives a 100 times reduction in relative error for the first 10 diameters of immersion. The second segment gives a 10 times further reduction in relative error for each additional 10 diameters of immersion. To reduce the immersion error below 0.001 % (1 mK at 120 °C, thermometers must be immersed to more than 40 diameters. Note that zero immersion corresponds to the thermometer just touching the surface of the calibration fluid.

4 Conclusions

Section 2 develops an improved mathematical model of the immersion characteristics of thermometers. The relative temperature error due to poor immersion decreases exponentially with increasing immersion with a dependence on two exponential decay terms. One of the exponential terms decays three times faster than the other, and is most significant for shallow immersion. For large immersions, a model with a single exponential term is sufficient.

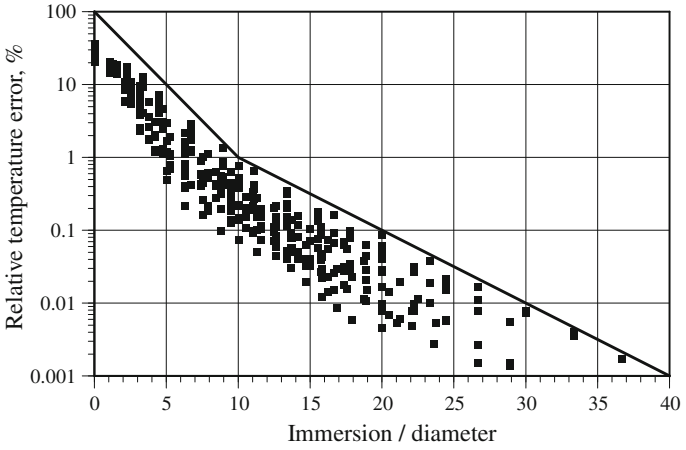

Fig. 6 All the immersion data for all the five IPRTs in the oil baths, with the immersion expressed in multiples of the IPRT diameter. The line gives an approximate upper bound to the relative temperature error

The mathematical model indicates that the 1/e decay length depends as much on the thermal environment (through the surface heat transfer coefficient) as on the thermometer itself. For stainless-steel sheathed industrial platinum resistance thermometers immersed in either mineral, silicon oil, or molten nitrate salt, the primary 1/e decay length was found to be three to four times the diameter of the thermometers, and surprisingly similar for all three fluids. The 1/e decay length of (3 to 4) diameters is longer than the 2.5 diameters found for a probe of similar construction immersed in a dry-block calibrator.

In fluid calibration baths, the surface heat transfer coefficient is dominated by a boundary layer effect that depends on the thermal conductivity, heat capacity, flow velocity, viscosity, and orientation of flow relative to the thermometer. Significant variability in the 1/e decay lengths was found for the larger diameter thermometers, possibly caused by neighboring thermometers in the calibration baths or the walls of the baths influencing the formation of boundary layers. The immersion characteristics for a thermometer therefore depend on both the structure and the fluid flow rates in the calibration bath.

For the measurements reported here it was found that the first 10 diameters of immersion ensured the relative temperature error is <1 %, and each additional 10 diameters of immersion further reduced the error by at least a factor of ten.

References

1. T.W. Kerlin, R.L. Shepard, *Industrial Temperature Measurement* (ISA, Research Triangle Park, 1982)
2. J.W. Nicholas, D.R. White, *Traceable Temperatures*. DSIR Bulletin, vol. 234 (DSIR, Wellington, 1982)
3. R.P. Benedict, J.W. Murdock, ASME Trans., J. Eng. Power 235 (1963)
4. M. Kutz, *Temperature Control* (Wiley, New York, 1968)
5. F.P. Incropera, D.P. DeWitt, *Fundamentals of Heat and Mass Transfer*, 4th edn. (Wiley, New York, 1996)
6. T.D. McGee, *Principles and Methods of Temperature Measurement* (Wiley, New York, 1998)